2019 18th European Control Conference (ECC)
Napoli, Italy, June 25-28, 2019

Practical differentiation using ultrasensitive molecular circuits

Christian Cuba Samaniego[1], Giulia Giordano[2] and Elisa Franco[3]

Abstract— **Biological systems compute spatial and temporal gradients with a variety of mechanisms, some of which have been shown to include integral feedback. In traditional engineering fields, it is well known that integral components within a negative feedback loop can be used to perform a derivative action. In this paper, we define the concept of a practical differentiator that is inspired by this design principle. We then consider three simple biological circuit examples in which we prove that feedback combined with ultrasensitive, quasi-integral components yields a practical differential network under some assumptions. These examples include phosphorylation/dephosphorylation cycles, and two networks relying on molecular sequestration.**

I. Introduction and motivation

Living organisms must respond to time varying environmental inputs to survive: for example, through the well-known mechanism of chemotaxis, many bacteria can sense and respond not only to the presence of nutrients but also to nutrient gradients [1]. To sense temporal or spatial gradients, cells compute an empirical derivative. Thus, a natural question for synthetic biologists is to identify minimal molecular mechanisms for derivative computation, useful to build more powerful and precise molecular sensors and controllers. Yet, few studies, such as [2] in a nonlinear setting, have focused on the synthesis of derivative molecular components. The linearized dynamics of a rapid buffering process have been shown to be mathematically equivalent to derivative negative feedback and improve stability of a closed loop system with limited sensitivity to molecular noise [3]. An approximate derivative component for PID controllers was computationally considered in [4] by operating near saturation a two node network that achieves perfect adaptation [5], [6], [7], [8]. A model for genetic differentiation that combines two genetic elements tracking positive and negative slopes of an input, and computes their difference via molecular sequestration, was also proposed and numerically studied in [9].

In traditional engineering fields, it is well known that an ideal integral block within a negative feedback loop can compute the derivative of the input (see block diagram in Fig. 1A); this idea was used to build the artificial genetic differentiator model described in [9]. This principle has also been identified in some natural biological networks underlying gradient computation, although their complexity makes it difficult to identify the essential reactions required. This is well illustrated by the chemotaxis example [10], [11], where the presence of a "hidden" integrator within a feedback loop enables the network adaptive properties [1], [6], [12]. Here, we propose that molecular gradient computation can be achieved in the presence of an *ultrasensitive reaction network within a feedback loop*.

Our idea is supported by the example of chemotaxis, illustrated in Fig. 1B. The chemical stimulus U binds to specialized receptors (MCPs), forming a stable complex with proteins CheW, not shown in the schematic, and CheA. The phosphorylated kinase CheA-P (active state) phosphorylates two downstream proteins CheY and CheB (both are constitutively inactive). As U increases, it generates CheA-P, marked as the output Y of the gray box, and indirectly increases the concentration of both CheY-P and CheB-P. In turn, CheY-P promotes tumbling by binding to the flagellar motor (CheY-P is dephosphorylated by CheZ). At the same time, CheB-P demethylates the MCPs, which take their inactive form MCPs*, introducing negative feedback. CheR, marked as the input R to the orange box, has an oppositive effect and methylates the receptor MCPs*. When CheR works at saturation and CheB works only on the active form of MCPs, the system achieves robust adaptation [1]. Because of its saturated operation, there is an *ultrasensitive* relationship between CheA-P (Y) and the fraction of active MCPs[13], [14], [15]. The ultrasensitive map is also tunable: when the concentration of CheR (R) changes, the threshold of the ultrasensitive input-output map is shifted [14].

Building on this example, we ask whether a network like the block diagram in Fig. 1C can be used as a general motif for gradient computation. Orange and gray blocks in Fig. 1A, B, and C map qualitatively similar components. Our idea is also motivated by our recent work, in which we showed that ultrasensitive networks can achieve quasi-integral action within a negative feedback loop [16]; here, we examine their capacity to achieve gradient computation.

We define the concept of a practical differentiator, and we examine three ultrasensitive reaction motifs that, when used within a feedback loop, operate as practical differentiators. These motifs include few species and reactions: in particular they rely on molecular sequestration and on enzymatic activation/deactivation cycles, which are very common reactions in nature. Thus, we envision that an experimental implementation of the proposed mechanisms is feasible. We support our analytical findings with numerical simulations that use biologically plausible parameters and concentrations.

Work partially supported by the National Science Foundation through grant CMMI-1266402 to EF, and by the Aspasia Grant and the DTF Grant at TU Delft to GG.

[1]Biodesign Center for Biocomputing, Security & Society at Arizona State University, and Department of Biological Engineering at Massachusetts Institute of Technology. ccubasam@mit.edu

[2]Delft Center for Systems and Control, Delft University of Technology, 2628 CD Delft, The Netherlands. g.giordano@tudelft.nl

[3]Department of Mechanical and Aerospace Engineering, University of California Los Angeles, California 90095, USA. efranco@seas.ucla.edu

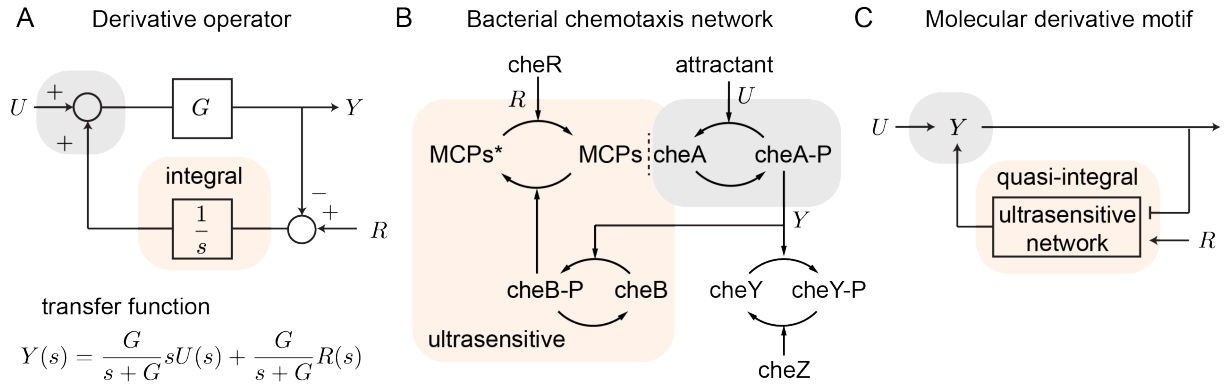

Fig. 1. **Networks that achieve derivative action** Orange and gray blocks identify network components having similar function in each example. A) An integral element within a negative feedback loop is a well known approach to achieve derivative action in linear systems. B) Bacterial chemotaxis computes a chemical gradient and allows cells to move toward sources of nutrients. The subnetwork marked in orange has an ultrasensitive behavior when mapping the relation between CheA-P (Y) and MCPs. C) We propose a motif for computation of molecular gradients that relies on ultrasensitive components within a negative feedback loop. The ultrasensitive network element is expected to have a function similar to the integrator in panel A (orange block).

II. Differentiator Motifs: Models and Analysis

We present different biomolecular network motifs that implement a practical differentiator system: in ideal conditions, the concentration of the output species is directly proportional to the time derivative of the input species.

We denote chemical species with uppercase letters, their concentrations with the corresponding lowercase letter; the corresponding uppercase letter also denotes the Laplace transform of a time signal, but the dependency on the Laplace variable s is then specified to avoid ambiguities.

Both first order [9] and second order low-pass filters are commonly used for practical differentiation. Low-pass filters of an arbitrary order could be adopted: the higher the order, the better the attenuation at high frequencies, which improves disturbance rejection. Second order low-pass filters are typically chosen as a compromise between simplicity and disturbance-rejecting cutoff frequency, hence we define a practical differentiator as follows.

Definition 1: A linear system with output $y(t)$ and input $u(t)$ is a *practical differentiator* if, denoting by $Y(s)$ and $U(s)$ the Laplace-transformed output and input, respectively (and setting all other inputs to zero), their ratio is described by a transfer function of the form

$$\frac{Y(s)}{U(s)} = \frac{ks}{s^2 + hs + g}, \tag{1}$$

where k, h and g are strictly positive numbers. ◇

Since in the transfer function (1) all the coefficients of the second-degree denominator polynomial are positive, both poles must have a negative real part and stability is guaranteed. The zero at $s = 0$ ensures that (1) can approximate very well a derivative action for low enough frequencies.

Next, we discuss three biomolecular network motifs that can behave as practical differentiators.

A. Post-translation enzymatic modification cycle

Consider a biomolecular network representing a generic post-translation enzymatic modification cycle; many proteins require covalent modifications to become functional, and these modifications are mediated by other proteins or enzymes. A well-known example is given by phosphorylation and dephosphorylation cycles, ubiquitous in eukaryotes. We show that, in combination with a negative feedback loop, this network can operate as a practical differentiator.

The core of the network is a molecular species that can be either active, Z, or inactive, Z^*, and whose total concentration is constant: $z + z^* = z^{tot}$. For example, activation of Z may occur through phosphorylation, and its inactivation through dephosphorylation. Species R, for example a kinase, binds to Z^* with a dissociation constant $\kappa^* > 0$, thus producing Z at a constant rate $\alpha > 0$. Species Y, for instance a phosphatase, yields Z^* at a constant rate $\theta > 0$ by binding to Z with a dissociation constant $\kappa > 0$. Additionally, both Z and Z^* degrade at rate $\xi \geq 0$. The active species Z drives a downstream process that produces Y at a constant rate $\beta > 0$, species U produces Y at a constant rate $\rho > 0$, while Y self-degrades at a constant rate $\delta > 0$. The schematic is visualised in Fig. 2 and the resulting dynamical model is

$$\dot{z} = \alpha \frac{r z^*}{z^* + \kappa^*} - \theta \frac{y z}{z + \kappa} - \xi z, \tag{2}$$

$$\dot{y} = \beta z + \rho u - \delta y, \tag{3}$$

where $z^* = z^{tot} - z$. The phosphorylation/dephosphorylation model we consider is consistent with previous examples in the literature [17].

We assume that the enzymes work in the saturation regime, resulting in an ultrasensitive steady-state response of equation (2) (input Y and output Z) [18].

Assumption 1: In system (2)–(3), $\frac{\kappa^*}{z^*}, \frac{\kappa}{z} \ll 1$. ◇

Under Assumption 1, the additive terms κ and κ^* in the denominators of the fractional functions in (2) are negligible and the equations (2)–(3) above can be rewritten as

$$\dot{z} = \alpha r - \theta y - \xi z \tag{4}$$

$$\dot{y} = \beta z + \rho u - \delta y \tag{5}$$

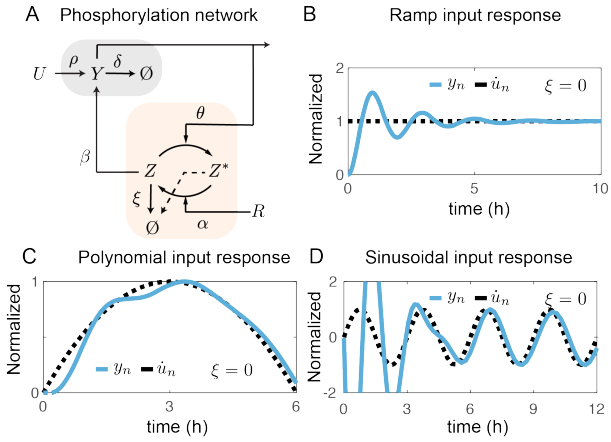

Fig. 2. **Post-translation modification cycle for gradient computation** A) Schematic of the network with inputs R and U and output Y. The network inside the orange box is an ideal integral controller when $\xi = 0$. B) Ramp response, $u(t) = At$, results in a constant output, where $A = 20$ nM/h . C) The input response of a polynomial, $u(t) = A(3T/2-t)t^2$ with derivative of a second order $\dot{u}(t) = 3At(T-t)$, where $A = 1.67$ nM, $T = 6$h. D) Input response to a period input, $u(t) = 0.5A(1+\sin(2\pi t/T - \pi/2))$, and derivative, $\dot{u}(t) = A\pi/T\cos(2\pi t/T - \pi/2)$, where $A = 50$ nM, $T = 3$h. We normalized $y(t)$ by subtracting the reference input $r = 500$ nM; $\dot{u}$ was normalized by dividing it by either its maximum value or by its steady state amplitude.

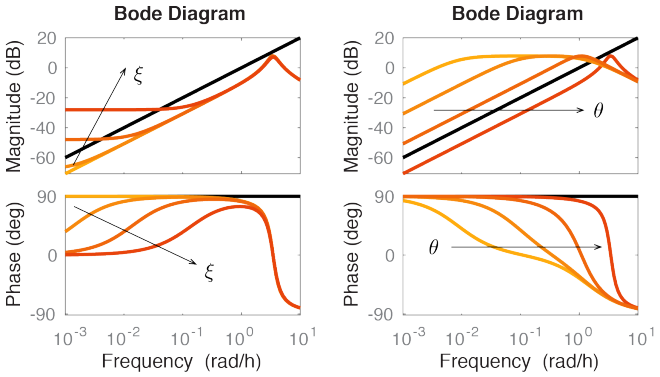

Fig. 3. **Frequency Analysis** Bode diagram (magnitude and phase) of an ideal derivative transfer function (black) and of $F_{U(s)\to Y(s)}$ with ξ proportional to $0, 10^{-3}, 10^{-2}, 10^{-1}$ times its nominal value (left) and θ proportional to $10^{-3}, 10^{-2}, 10^{-1}, 1$ times its nominal value (right), increasing from yellow to red. Decreasing ξ increases the frequency range where the system works as a practical differentiator (left), since the lower frequency bound for working conditions is decreased. Also, increasing θ leads to an increase in the upper frequency bound for working conditions (right).

When the modification rates are faster than degradation rate ξ, the ultrasensitive steady-state behavior of equation (2) is enhanced [18]. In our case, given the order of magnitude of biologically reasonable parameters, $\alpha, \theta \gg \xi$, we can make the following assumption.

Assumption 2: In system (2)–(3), $\xi = 0$. ◇

We can now prove that, under Assumptions 1 and 2, the network implements a molecular differentiator.

Proposition 1: If Assumption 2 holds, the linear system (4)–(5), with output $y(t)$ and input $u(t)$, is a practical differentiator network according to Definition 1. □

Proof. To show that $y(t)$ is a function of $\dot{u}(t)$, it is convenient to take the Laplace transform of the equations (4)–(5) and write $Y(s)$ as a function of $R(s)$ and $U(s)$. The resulting transfer function is:

$$\begin{aligned} Y(s) &= \frac{\alpha\beta}{s^2 + (\delta+\xi)s + \beta\theta + \delta\xi} R(s) \\ &+ \frac{\rho(s+\xi)}{s^2 + (\delta+\xi)s + \beta\theta + \delta\xi} U(s), \end{aligned}$$

where the first term depends on the "molecular reference" $R(s)$, while the second term depends on the input $U(s)$. Since all its coefficients are positive, the second-degree characteristic polynomial is Hurwitz, as required. In the presence of degradation, the system is not a practical differentiator: the second term includes both a derivative and a proportional action. However, under Assumption 2, $\xi = 0$ and the transfer function becomes

$$Y(s) = \frac{\alpha\beta}{s^2 + \delta s + \beta\theta} R(s) + \frac{\rho s}{s^2 + \delta s + \beta\theta} U(s), \qquad (6)$$

where all the coefficients of the characteristic polynomial are positive, hence the relation between $Y(s)$ and $U(s)$ matches that in Definition 1. ■

As discussed in the proof, both the transfer functions $F_{R(s)\to Y(s)}$ and $F_{U(s)\to Y(s)}$ are stable (regardless of ξ being strictly positive or being zero). When $r(t) \equiv r$ is assumed to be constant and $u(t)$ is a generic signal, in the ideal case when $\xi = 0$ (no degradation), the network output $y(t)$ corresponds to the derivative $\dot{u}(t)$, suitably shifted depending on r. As Fig. 3 shows, when $\xi = 0$, for a large low-frequency range the transfer function $F_{U(s)\to Y(s)}$ behaves exactly as an ideal differentiator, as expected: its magnitude increases with slope 20 dB/dec and its phase is $\pi/2$. As stated in Assumption 2, the rates α and θ are much larger than the other parameters. This allows the transfer function to be comparable to an ideal differentiator for a larger range of frequencies: indeed when $\xi = 0$, as shown in Fig. 3 (right), the larger θ, the broader the interval in which the magnitude increases with slope 20 dB/dec and the phase is $\pi/2$: increasing θ increases the upper frequency bound for the system to work as a practical differentiator. Conversely, in the presence of a degradation $\xi \neq 0$, then the transfer function from $U(s)$ to $Y(s)$ does not include just a derivative action, but also a proportional action, which leads to a different outcome for low frequencies, as can be seen in Fig. 3 (left). Hence, decreasing ξ increases the frequency range for the system to work as a practical differentiator, by decreasing the lower frequency bound.

B. Molecular sequestration

Here we study a network for practical differentiation that is based on molecular sequestration (or titration). In biology, sequestration is a versatile mechanism that can enable ultrasensitivity [19], [20]. This type of reaction operates in a manner similar to an electronic diode with a tunable threshold, and helps extracting the minimum of two

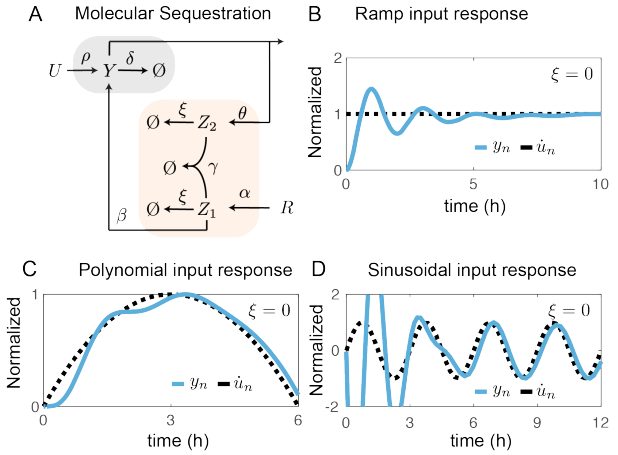

Fig. 4. **Molecular sequestration network for gradient computation** A) Schematic of the molecular sequestration network. B) Ramp response, $u(t) = At$, results in a constant output, where $A = 20$ nM/h. C) The input response of a polynomial, $u(t) = A(3T/2 - t)t^2$ with derivative of a second order $\dot{u}(t) = 3At(T - t)$, where $A = 1.67$ nM, $T = 6$h. D) Input response to a period input, $u(t) = 0.5A(1 + \sin(2\pi t/T - \pi/2))$, and derivative, $\dot{u}(t) = A\pi/T\cos(2\pi t/T - \pi/2)$, where $A = 50$ nM, $T = 3$h. We normalized $y(t)$ by subtracting the reference input $r = 500$ nM; $\dot{u}$ was normalized by dividing it by either its maximum value or by its steady state amplitude.

inputs [21] and compute errors [22], [21]. Sequestration can generally compute the difference between signals [23], and was previously exploited to propose a model for a genetic differentiator [9].

Our model ultrasensitive network is built around two chemical species, Z_1 and Z_2, which are produced at constant rates α and θ by species R and Y, respectively, and degrade at a constant rate ξ. Species Z_1 and Z_2 sequester each other at a constant *titration rate* γ: they bind to form a waste complex. Species Z_1 drives a downstream process that produces at a constant rate β species Y, which degrades at a constant rate δ. Also U produces Y at a constant rate ρ. The network schematic is in Fig. 4, and the resulting system of ordinary differential equations is

$$\begin{aligned} \dot{z}_1 &= \alpha r - \gamma z_1 z_2 - \xi z_1 && (7)\\ \dot{z}_2 &= \theta y - \gamma z_1 z_2 - \xi z_2 && (8)\\ \dot{y} &= \beta z_1 + \rho u - \delta y. && (9) \end{aligned}$$

If the titration rate γ is large, the input Y to output Z_1 steady state mapping of equations (7) and (8) is ultrasensitive, and the static gain is proportional to the ratio between production and degradation rate constants [19], [20]. In view of the order of magnitude of biologically reasonable parameters, $\alpha, \theta, \gamma \gg \xi$, we can make the following assumption.

Assumption 3: In system (7)–(9), $\xi = 0$. ◇

If the decay rate $\xi = 0$, it has been shown that molecular sequestration can be used to build an ideal integral controller, also known as Antithetic Integral Controller (AIC) [24]. (Quasi-integral behavior and steady-state ultrasensivitiy can be achieved when the production rates are larger than degradation [25], [16].)

If the titration rate γ is very large, and the amount of Z_1 is much larger than that of Z_2, then z_2 converges very quickly to its steady-state value, hence $\dot{z}_2 = 0$ [26], [27].

Assumption 4: In system (7)–(9), $\dot{z}_2 = 0$. ◇

Proposition 2: Under Assumptions 3 and 4, the system (7)–(9), with output $y(t)$ and input $u(t)$, is a practical differentiator network according to Definition 1. □

Proof. When $\xi = 0$ according to Assumption 3 and $\dot{z}_2 = 0$ according to Assumption 4, then system (7)–(9) becomes a linear system:

$$\begin{aligned} \dot{z}_1 &= \alpha r - \gamma z_1 z_2 = \alpha r - \theta y && (10)\\ 0 &= \theta y - \gamma z_1 z_2 && (11)\\ \dot{y} &= \beta z_1 + \rho u - \delta y. && (12) \end{aligned}$$

To show that $y(t)$ is a function of $\dot{u}(t)$, we take the Laplace transform of the equations:

$$Y(s) = \frac{\alpha\beta}{s^2 + \delta s + \beta\theta} R(s) + \frac{\rho s}{s^2 + \delta s + \beta\theta} U(s), \quad (13)$$

where all the coefficients of the characteristic polynomial are positive (which guarantees stability), hence the relation between $Y(s)$ and $U(s)$ matches that in Definition 1. ■

Note that (13) has exactly the same form as (6), hence the same considerations as in the previous case apply.

However, the relations in the non-ideal case (in which Assumption 2 does not hold for the post-translational network discussed previously, and Assumptions 3 and 4 do not hold for the molecular sequestration network) are different: in the case of the sequestration network, there is an additional term introducing an offset that depends on Z_2.

C. A synthetic, tunable ultrasensitive network

Here we study a biomolecular network that combines the two reaction motifs examined in the previous sections, the post-translational cycle motif and molecular sequestration. We note that when these motifs are combined, it is no longer necessary to require that the post-translational cycle motif operates at saturation to achieve an ultrasensitive steady-state input-output map. Networks with a similar structure are very versatile and can be tuned to generate bistable dynamics [28], [29], oscillations [30], [31], and molecular quasi-integral controllers [16], [32]. Here we show that, under certain assumptions, this motif can also serve as a practical differentiator.

The first component of the network is the sequestration motif, which is composed of two chemical species, Z_1 and Z_2; these species are produced at constant rates α and θ by species R and Y, respectively, and degrade at a constant rate ϕ. These two species Z_1 and Z_2 can sequester each other at a constant rate γ and form a waste complex. The second component of the network is an enzymatic cycle: a species can be present both in an active state, Z, and an inactive state, Z^*, while its total concentration is constant: $z + z^* = z^{tot}$. Species Z_1 can activate Z^* at a constant rate κ, while species Z_2 can inactivate Z at the same rate. Species Z and Z^* degrade at a constant rate ξ; Z (active state) drives a downstream process that produces at a constant

rate β species Y, which also degrades at a constant rate δ. Species U produces Y at a constant rate ρ. The network is sketched in Fig. 5, and the resulting system of ordinary differential equations is

$$\begin{aligned} \dot{z}_1 &= \alpha r - \gamma z_1 z_2 - \kappa z_1 z^* - \phi z_1 && (14)\\ \dot{z}_2 &= \theta y - \gamma z_1 z_2 - \kappa z_2 z - \phi z_2 && (15)\\ \dot{z} &= \kappa z_1 z^* - \kappa z_2 z - \xi z && (16)\\ \dot{y} &= \beta z + \rho u - \delta y. && (17) \end{aligned}$$

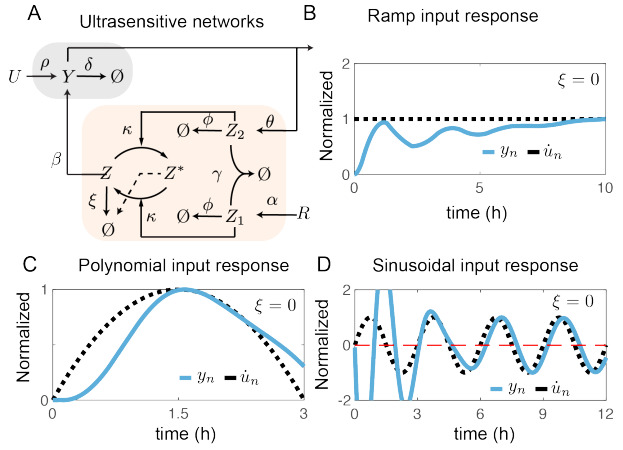

Fig. 5. **Ultrasensitive network for gradient computation** A) Schematic of the Brink network. B) Ramp response, $u(t) = At$, results in a constant output, where $A = 0.6$ nM/h. C) The input response of a polynomial, $u(t) = A(3T/2 - t)t^2$ with derivative of a second order $\dot{u}(t) = 3At(T - t)$, where $A = 1.67$ nM, $T = 6$h. D) Input response to a period input, $u(t) = 0.5A(1 + \sin(2\pi t/T - \pi/2))$, and derivative, $\dot{u}(t) = A\pi/T\cos(2\pi t/T - \pi/2)$, where $A = 50$ nM, $T = 3$h. We normalized $y(t)$ by subtracting the reference input $r = 500$ nM; $\dot{u}$ was normalized by dividing it by either its maximum value or by its steady state amplitude.

The subnetwork comprised of equations (14), (15) and (16), exhibits an ultrasensitive input-output behaviour (input Y, output Z) when κ and γ are very large [16], [33]. We focus our analysis on this regime. Since $\kappa \gg \xi$, we can assume the following.

Assumption 5: In system (14)–(17), $\xi = 0$. ◇

Also, when $\gamma \gg \phi$, ϕ can be neglected. Moreover, if γ is very large, molecular sequestration between Z_1 and Z_2 is fast and these species reach their steady-state concentration very quickly. Hence, in view of time-scale separation arguments, we can assume that $\dot{z}_1$ and $\dot{z}_2$ are zero.

Assumption 6: In system (14)–(17), $\phi = 0$, and also $\dot{z}_1 = \dot{z}_2 = 0$. ◇

Proposition 3: Under Assumptions 5 and 6, the system (14)–(17), with output $y(t)$ and input $u(t)$, is a practical differentiator network according to Definition 1. □

Proof. When $\phi = 0$ and $\dot{z}_1 = \dot{z}_2 = 0$ according to Assumption 6 and $\xi = 0$ according to Assumption 5, then system (14)–(17) becomes a linear system:

$$\begin{aligned} 0 &= \alpha r - \gamma z_1 z_2 - \kappa z_1 z^* && (18)\\ 0 &= \theta y - \gamma z_1 z_2 - \kappa z_2 z && (19)\\ \dot{z} &= \kappa z_1 z^* - \kappa z_2 z = \alpha r - \theta y && (20)\\ \dot{y} &= \beta z + \rho u - \delta y && (21) \end{aligned}$$

Hence, the Laplace transform yields

$$Y(s) = \frac{\alpha\beta}{s^2 + \delta s + \beta\theta} R(s) + \frac{\rho s}{s^2 + \delta s + \beta\theta} U(s), \quad (22)$$

where all the coefficients of the characteristic polynomial are positive (which guarantees stability), hence the relation between $Y(s)$ and $U(s)$ matches that in Definition 1. ■

Note again that, although in the non-ideal case the relations for all the systems considered so far are different (here there is an additional term depending on $z_1 - z_2$ that introduces another offset), the ideal relation is the same: (22) has exactly the same form as (6) and (13), hence the same considerations as in the previous cases apply.

III. Numerical Simulations

Throughout the paper, deterministic simulations were done by integrating ODE models using MATLAB, using the parameters listed in Table I.

TABLE I
NOMINAL SIMULATION PARAMETERS OF THE CONTROLLED SYSTEM

Parameter	Description	Value	Other studies
$\alpha, \theta, \beta, \rho$ (/s)	Production	$9.5.10^{-4}$	$2.710^{-4} - 1$ [34], [35] [36], [37]
γ (/M/s)	Titration	$2.1 \cdot 10^5$	$10^4 - 10^6$ [38], [39]
ϕ, δ, ξ (/s)	Degradation	$1.2 \cdot 10^{-3}$	$10^{-4} - 10^{-3}$ [40].

IV. Conclusion

We have presented a strategy to build molecular networks that operate as practical differentiators; the strategy relies on the use of an ultrasensitive element within a negative feedback loop. We provide three implementation examples, in which we use ultrasensitive components that are common in synthetic biology. We discuss critical assumptions on the network parameters to achieve ultrasensitivity, and we report numerical simulations supporting our proofs. Two of the network motifs we examined include molecular sequestration, which has been previously exploited to compute the difference between signals [23], [9].

Gradient computation is essential for the survival of biological organisms; our design principle takes direct inspiration from the classical example of chemotaxis, which allows bacteria to search regions in which nutrients are more abundant. We believe that simple, general principles for designing gradient computation will help advance the capabilities of spatial and temporal control of engineered molecular networks in natural and synthetic cells.

REFERENCES

[1] N. Barkai and S. Leibler, "Robustness in simple biochemical networks," *Nature*, vol. 387, no. 6636, p. 913, 1997.

[2] M. Lang and E. Sontag, "Scale-invariant systems realize nonlinear differential operators," in *2016 American Control Conference*, 2016, pp. 6676–6682.

[3] E. J. Hancock, J. Ang, A. Papachristodoulou, and G.-B. Stan, "The interplay between feedback and buffering in cellular homeostasis," *Cell systems*, vol. 5, no. 5, pp. 498–508, 2017.

[4] M. Chevalier, M. Gomez-Schiavon, A. Ng, and H. El-Samad, "Design and analysis of a Proportional-Integral-Derivative controller with biological molecules," *bioRxiv*, p. 303545, 2018.

[5] P. A. Spiro, J. S. Parkinson, and H. G. Othmer, "A model of excitation and adaptation in bacterial chemotaxis," *Proceedings of the National Academy of Sciences*, vol. 94, no. 14, pp. 7263–7268, 1997.

[6] T.-M. Yi, Y. Huang, M. I. Simon, and J. Doyle, "Robust perfect adaptation in bacterial chemotaxis through integral feedback control," *Proceedings of the National Academy of Sciences*, vol. 97, no. 9, pp. 4649–4653, 2000.

[7] T. Drengstig, H. R. Ueda, and P. Ruoff, "Predicting perfect adaptation motifs in reaction kinetic networks," *The Journal of Physical Chemistry B*, vol. 112, no. 51, pp. 16 752–16 758, 2008.

[8] S. Waldherr, S. Streif, and F. Allgöwer, "Design of biomolecular network modifications to achieve adaptation," *IET Systems Biology*, vol. 6, no. 6, pp. 223–231, 2012.

[9] W. Halter, Z. A. Tuza, and F. Allgöwer, "Signal differentiation with genetic networks," *IFAC-PapersOnLine*, vol. 50, no. 1, pp. 10 938–10 943, 2017.

[10] D. A. Clark and L. C. Grant, "The bacterial chemotactic response reflects a compromise between transient and steady-state behavior," *Proceedings of the National Academy of Sciences*, vol. 102, no. 26, pp. 9150–9155, 2005.

[11] A. Celani and M. Vergassola, "Bacterial strategies for chemotaxis response," *Proceedings of the National Academy of Sciences*, vol. 107, no. 4, pp. 1391–1396, 2010.

[12] P. A. Iglesias and P. N. Devreotes, "Navigating through models of chemotaxis." *Current opinion in cell biology*, vol. 20 1, pp. 35–40, 2008.

[13] U. Roy and M. Gopalakrishnan, "Ultrasensitivity and fluctuations in the barkai-leibler model of chemotaxis receptors in escherichia coli," *PloS one*, vol. 12, no. 4, p. e0175309, 2017.

[14] Y. Tu, T. S. Shimizu, and H. C. Berg, "Modeling the chemotactic response of escherichia coli to time-varying stimuli," *Proceedings of the National Academy of Sciences*, vol. 105, no. 39, pp. 14 855–14 860, 2008.

[15] J. Yuan and H. C. Berg, "Ultrasensitivity of an adaptive bacterial motor," *Journal of molecular biology*, vol. 425, no. 10, pp. 1760–1764, 2013.

[16] C. Cuba Samaniego and E. Franco, "Ultrasensitive molecular controllers for quasi-integral feedback," *bioRxiv*, p. 413914, 2018.

[17] D. Angeli, J. E. Ferrell, and E. D. Sontag, "Detection of multistability, bifurcations, and hysteresis in a large class of biological positive-feedback systems," *Proceedings of the National Academy of Sciences of the USA*, vol. 101, no. 7, pp. 1822–1827, 2004.

[18] A. Goldbeter and D. E. Koshland, "An amplified sensitivity arising from covalent modification in biological systems," *Proceedings of the National Academy of Sciences*, vol. 78, no. 11, pp. 6840–6844, 1981.

[19] N. E. Buchler and M. Louis, "Molecular titration and ultrasensitivity in regulatory networks," *Journal of molecular biology*, vol. 384, no. 5, pp. 1106–1119, 2008.

[20] C. Cuba Samaniego, G. Giordano, J. Kim, F. Blanchini, and E. Franco, "Molecular titration promotes oscillations and bistability in minimal network models with monomeric regulators," *ACS synthetic biology*, vol. 5, no. 4, pp. 321–333, 2016.

[21] H. Steel, A. W. Harris, E. J. Hancock, C. L. Kelly, and A. Papachristodoulou, "Frequency domain analysis of small non-coding rnas shows summing junction-like behaviour," in *Decision and Control (CDC), 2017 IEEE 56th Annual Conference on*. IEEE, 2017, pp. 5328–5333.

[22] D. K. Agrawal, E. Franco, and R. Schulman, "A self-regulating biomolecular comparator for processing oscillatory signals," *Journal of The Royal Society Interface*, vol. 12, no. 111, p. 20150586, 2015.

[23] K. Oishi and E. Klavins, "Biomolecular implementation of linear I/O systems," *IET Systems Biology*, vol. 5, no. 4, pp. 252–260, 2011.

[24] C. Briat, A. Gupta, and M. Khammash, "Antithetic integral feedback ensures robust perfect adaptation in noisy biomolecular networks," *Cell systems*, vol. 2, no. 1, pp. 15–26, 2016.

[25] Y. Qian and D. Del Vecchio, "Realizing integral control in living cells: how to overcome leaky integration due to dilution?" *Journal of The Royal Society Interface*, vol. 15, no. 139, p. 20170902, 2018.

[26] M. Del Giudice, C. Bosia, S. Grigolon, and S. Bo, "Stochastic sequestration dynamics: a minimal model with extrinsic noise for bimodal distributions and competitors correlation," *Scientific reports*, vol. 8, no. 1, p. 10387, 2018.

[27] N. Olsman, A.-A. Baetica, F. Xiao, Y. P. Leong, J. Doyle, and R. Murray, "Hard limits and performance tradeoffs in a class of sequestration feedback systems," *bioRxiv*, p. 222042, 2018.

[28] C. Cuba Samaniego, H. K. Subramanian, and E. Franco, "Design of a bistable network using the crispr/cas system," in *Control Technology and Applications (CCTA), 2017 IEEE Conference on*. IEEE, 2017, pp. 973–978.

[29] V. Mardanlou, C. Cuba Samaniego, and E. Franco, "A bistable biomolecular network based on monomeric inhibition reactions," in *Decision and Control (CDC), 2015 IEEE 54th Annual Conference on*. IEEE, 2015, pp. 3858–3863.

[30] C. Cuba Samaniego, S. Kitada, and E. Franco, "Design and analysis of a synthetic aptamer-based oscillator," in *American Control Conference (ACC), 2015*. IEEE, 2015, pp. 2655–2660.

[31] C. Cuba Samaniego, G. Giordano, F. Blanchini, and E. Franco, "Stability analysis of an artificial biomolecular oscillator with non-cooperative regulatory interactions," *Journal of biological dynamics*, vol. 11, no. 1, pp. 102–120, 2017.

[32] C. Cuba Samaniego and E. Franco, "An ultrasensitive biomolecular network for robust feedback control," *IFAC-PapersOnLine*, vol. 50, no. 1, pp. 10 950–10 956, 2017.

[33] C. Cuba-Samaniego and E. Franco, "An ultrasensitive motif for robust closed loop control of biomolecular systems," in *Decision and Control (CDC), 2017 IEEE 56th Annual Conference on*. IEEE, 2017, pp. 5334–5340.

[34] R. Hussein and H. N. Lim, "Direct comparison of small RNA and transcription factor signaling," *Nucleic acids research*, vol. 40, no. 15, pp. 7269–7279, 2012.

[35] R. Milo and R. Phillips, *Cell biology by the numbers*. Garland Science, 2015.

[36] U. Vogel and K. F. Jensen, "The RNA chain elongation rate in *Escherichia coli* depends on the growth rate," *Journal of Bacteriology*, vol. 176, no. 10, pp. 2807–2813, 1994.

[37] H. Chen, K. Shiroguchi, H. Ge, and X. S. Xie, "Genome-wide study of mRNA degradation and transcript elongation in *Escherichia coli*," *Molecular systems biology*, vol. 11, no. 1, p. 781, 2015.

[38] J. Kim, K. S. White, and E. Winfree, "Construction of an *in vitro* bistable circuit from synthetic transcriptional switches," *Molecular systems biology*, vol. 2, no. 1, p. 68, 2006.

[39] D. Y. Zhang, A. J. Turberfield, B. Yurke, and E. Winfree, "Engineering entropy-driven reactions and networks catalyzed by DNA," *Science*, vol. 318, no. 5853, pp. 1121–1125, 2007.

[40] J. Kim, I. Khetarpal, S. Sen, and R. M. Murray, "Synthetic circuit for exact adaptation and fold-change detection," *Nucleic acids research*, p. gku233, 2014.